Identification of SAMT family proteins as substrates of MARCH11 in mouse spermatids

Identification of SAMT family proteins as substrates of MARCH11 in mouse spermatids

Keiichiro Yogo[1], Hidehiro Tojima[1], Jun-ya Ohno[1], Takuya Ogawa[3], Nobuhiro Nakamura[2], Shigehisa Hirose[2], Tatsuo Takeya[3], and Tetsuya Kohsaka[1]

[1]Animal Reproduction and Physiology, Faculty of Agriculture, Shizuoka University, Shizuoka 422-8529, Japan

[2]Department of Biological Sciences, Tokyo Institute of Technology, Yokohama 226-8501, Japan

[3]Graduate School of Biological Sciences, Nara Institute of Science and Technology, Nara 630-0192, Japan

Correspondence to: Keiichiro Yogo, Animal Reproduction and Physiology, Faculty of Agriculture, Shizuoka University, 836 Ohya, Suruga, Shizuoka 422-8529, Japan.

Tel./Fax: 81-54-238-4868; E-mail: akyogo@ipc.shizuoka.ac.jp

Abstract

MARCH11, a RING-finger transmembrane ubiquitin ligase, is predominantly expressed in spermatids and localized to the trans-Golgi network (TGN) and multivesicular bodies (MVBs). Because ubiquitination acts as a sorting signal of cargo proteins, MARCH11 has been postulated to mediate selective protein sorting via the TGN-MVB pathway. However, the physiological substrate of MARCH11 has not been identified. In this study, we have identified and characterized SAMT1, a member of a novel 4-transmembrane protein family, which consists of 4 members. *Samt1* mRNA and its expression product were found to be specific to the testis and were first detected in germ cells 25 days after birth in mice. Immunohistochemical analysis further revealed that SAMT1 was specifically expressed in haploid spermatids during the cap and acrosome phases. Confocal microscopic analysis showed that SAMT1 co-localized with MARCH11 as well as with fucose-containing glycoproteins, another TGN/MVB marker, and LAPM2, a late endosome/lysosome marker. Furthermore, we found that MARCH11 could increase the ubiquitination of SAMT1 and enhance its lysosomal delivery and degradation in an E3 ligase activity-dependent manner. In addition, the C-terminal region of SAMT1 was indispensable for its ubiquitination and proper localization. The other member proteins of the SAMT family also showed similar expression profile, intracellular localization, and biochemical properties, including ubiquitination by MARCH11. These results suggest that SAMT family proteins are physiological substrates of MARCH11 and are delivered to lysosomes through the TGN-MVB pathway by a ubiquitin-dependent sorting system in mouse spermatids.

35 Keywords: spermatogenesis, multivesicular body, membrane trafficking, ubiquitination

Introduction

Mammalian spermatogenesis is a complex process that regulates the differentiation of spermatogonial stem cells into mature, haploid spermatozoa in the seminiferous epithelium of the testis. In the late phase of spermatogenesis, also called spermiogenesis, spermatids undergo dynamic morphological and biochemical changes such as axoneme and acrosome formation, nuclear elongation and condensation, and the shedding of residual bodies (Clermont 1972; Eddy 2002). These changes during differentiation are regulated by the highly organized actions of gene products that are expressed in a cell- and stage-specific manner (Eddy 2002; Tanaka and Baba 2005; Braun 1998).

Membrane trafficking is a fundamental cellular process and is essential for sperm morphogenesis and fertility. For instance, deficiency of GOPC (Golgi-associated PDZ- and coiled-coil motif-containing protein), a trans-Golgi network (TGN)-localized protein, results in abnormal spermatogenesis, including a lack of acrosome formation, nuclear malformation, and an abnormal arrangement of the mitochondria in mice, probably as a result of a defect in vesicle transport from the Golgi apparatus (Yao et al. 2002). A number of studies using electron microscopy and immunohistochemical techniques have shown that Golgi-derived vesicles are transported to 2 organelles. One of these is the acrosome, a secretory vesicle that contains a number of hydrolytic enzymes required for penetration of the egg envelope (Ramalho-Santos et al. 2002; Yoshinaga and Toshimori 2003; Hermo et al. 2010). Vesicle trafficking during acrosome formation has been extensively studied. The trafficking appears to be mediated by both clathrin-coated (Griffiths et al. 1981) and

COPI-coated vesicles (Martinez-Menarguez et al. 1996b). SNARE and Rab GTPases, which are essential components of the membrane fusion machinery, have also been found to associate with the acrosome (Moreno et al. 2000; Ramalho-Santos and Moreno 2001; Ramalho-Santos et al. 2001). The other destination organelle of TGN-derived vesicles is the multivesicular body (MVB) (Clermont and Tang 1985; Clermont et al. 1993). MVBs are a type of endosomes that possess a membrane-enclosed structure containing multiple intraluminal vesicles and are found in many cell types. In somatic cells and yeast, endocytosed plasma membrane proteins are first delivered to early endosomes. Afterward, some of the proteins are recycled back to the plasma membrane while others destined for degradation are sorted into the lumen by inward budding from the limiting membrane, which leads to the formation of MVBs. Finally, MVBs fuse with lysosomes, and the intraluminal vesicles are digested by lysosomal hydrolases (Piper and Katzmann 2007; Raiborg and Stenmark 2009). In spermatogenesis, more than one MVB per cell has commonly been found in pachytene spermatocytes (Haraguchi et al. 2004) and spermatids (Clermont and Tang 1985; Mollenhauer and Zebrun 1960), and MVBs have been often seen adjacent to the nucleus and the chromatoid body (Ventela et al. 2003; Haraguchi et al. 2005; Parvinen 2005). Then, MVBs accumulate at the centriolar pole of the nucleus and eventually disappear as spermatids mature (Clermont et al. 1993). The existence of MVBs in male germ cells was first described in 1960 (Mollenhauer and Zebrun 1960), but to date, little is known about the cargo proteins and the selective sorting mechanism involved in protein transport from the TGN to MVBs.

Recently, *March11*, a gene encoding a novel member of the transmembrane RING-finger ubiquitin ligases, has been isolated (Morokuma et al. 2007). MARCH11 is predominantly expressed in developing

spermatids in a stage-specific manner and is localized to TGN vesicles and MVBs (Morokuma et al. 2007). Because ubiquitination serves as a sorting signal for incorporation of target proteins into MVBs from the plasma membrane and the TGN, MARCH11 is postulated to mediate selective protein sorting via the TGN-MVB transport pathway through its ubiquitin ligase activity. However, the physiological function and target substrate(s) of MARCH11 remain to be identified.

In this study, to identify a novel membrane protein that functions in spermiogenesis, including membrane trafficking, we screened for spermatid-specific membrane protein genes in mice and isolated the *Samt1* gene, a member of a putative, 4-transmembrane protein family. We examined the *Samt1* expression profile, as well as the localization and functional relation between SAMT1 and MARCH11.

Materials and Methods

Animals

Mice (ICR and *W/W*^{v}) and rabbits were purchased from Japan SLC (Hamamatsu, Japan). All animal experiments were approved by the Institutional Animal Care and Use Committee of Shizuoka University.

Screening of membrane protein genes in silico

National Center for Biotechnology Information Gene Expression Omnibus (GEO) data sets

(GDS401, GDS409, GDS410, GDS605, GDS606, and GDS607) were searched for spermatogenesis-associated membrane protein genes. These data sets were derived from 2 comprehensive gene expression analyses of postnatal spermatogenesis in mouse testis with Affymetrix Murine Genome U74v2 A, B, and C arrays (Schultz et al. 2003; Shima et al. 2004). A group of genes that showed increased expression of 6-fold or more 20 days after birth were selected using the "Data Analysis Tools" in GEO, and their putative amino acids sequences were surveyed for the presence of transmembrane domain(s) by using the transmembrane helices prediction program TMHMM Server v. 2.0 (http://www.cbs.dtu.dk/services/TMHMM/). Subsequently, the expression profile of each gene was checked with the EST profile in the UniGene database. Genes specifically expressed in the testis were selected. Finally, 53 genes were obtained from the screening and identified as putative spermatogenesis-associated transmembrane protein genes. These included IZUMO1 and ADAM3, which are germ cell-specific membrane proteins (Inoue et al. 2005; Wolfsberg et al. 1995).

Reverse transcriptase-polymerase chain reaction

Total RNA was isolated from mouse tissues with ISOGEN (Nippongene). Five micrograms of total RNA was used as a template, and reverse transcription reactions were performed with ReverTra Ace reverse transcriptase (TOYOBO) according to the manufacturer's instructions. Polymerase chain reaction (PCR) was carried out under the following conditions: 94°C for 2 min; 30 cycles each of 94°C for 30 s, 59°C for 30 s, and 72°C for 60 s; and a final extension of 72°C for 7 min. The following primer pairs were used for the

expression analysis: *Samt1*, 5′-CTCTAACACTGGGCAGTCAC-3′ and 5′-GAGTTTCCTGTAGGAAGAGG-3′; *Samt2*, 5′-GAACTTCCTAGAAGAGACATA-3′ and 5′-TTACATGAGTACTGTGTGGTG-3′; *Samt3*, 5′-AGACCAGAGAAAGCCTTTGG-3′ and 5′-TAGTAATGTGTGCATACAGACAC-3′; *Samt4*, 5′-GCTAGAATCACATTTGGTTGTCAC-3′ and 5′-GACAGATGTTGGCTATGCAG-3′; *Gapdh*, 5′-CATCACCATCTTCCAGGAGCG-3′ and 5′-AAGGCCATGCCAGTGAGCTTC-3′. PCR products were analyzed by electrophoresis with 1.5% agarose gel, and signals were visualized by staining with ethidium bromide.

Antibodies

Rabbit polyclonal anti-SAMT1 antibody was raised against a KLH-conjugated peptide corresponding to the C-terminal region of mouse SAMT1 (^{222}RPVKANDASKMGLLDA^{237}). Following the second immunization, serum was collected, and the antibody was purified by affinity chromatography using an antigen peptide-conjugated column. Anti-ubiqutin mouse monoclonal antibody (P4D1), anti-GFP monoclonal antibody (JL-8), rat anti-LAMP2 antibody (ABL-93), anti-FLAG monoclonal antibody (M2), and anti-GM130 (clone 35) antibody were purchased from Santa Cruz Biotechnology, Clontech, eBioscience, Sigma, and BD Transduction Laboratories, respectively. Rabbit and rat anti-MARCH11 antibodies were generated as previously described (Morokuma et al. 2007).

Plasmids

A mouse *Samt1* cDNA fragment was obtained by PCR amplification with the primers 5′-GAATTCATGGATCAACTCATCGTTG-3′ and 5′-GGATCCGACGCATCTAGAAGGCCCATTTTG-3′ and cloned into T-vector pMD20 (TaKaRa). The *Eco*RI-*Bam*HI fragment was subcloned into the GFP-fusion protein expression vector pEGFP-N1 (Clontech) and the FLAG-tag expression vector pFLAG-N1, a vector modified from pEGFP-N1 by replacement of the GFP-coding region with the FLAG tag sequence. FLAG-tagged *Samt2*, *Samt3*, and *Samt4* expression vectors were similarly constructed using the following primers: *Samt2*, 5′-CTCGAGATGGATTGCTATACCCTCAAC-3′ and 5′-GAATTCTGGGAGTCTCCTGGCACATTTGGC-3′; *Samt3*, 5′-CTCGAGATGAATTTCCTCACCTGCG-3′ and 5′-CTGCAGTGTCTTTTGATTGATCAGTCTGG-3′; *Samt4*, 5′-CTCGAGATGGATCTCTTCACCCTTGATAC-3′ and 5′-GAATTCTGGCCTCTTGAAGGGCCACTTTG-3′. Mouse *March11* cDNA and human *Ubiqutin* cDNA were obtained by PCR and inserted into a pHM6 expression vector (Roche) and a pCMX vector (kindly provided by Dr. Umezono), respectively. *Samt1* C-terminal deletion mutant and *March11* RING-finger mutant (C171S, C184S, C186S), which lacks ligase activity, were constructed by PCR-based mutagenesis. All sequences were confirmed by sequence analysis.

Cell culture and transfection

293F cells (Invitrogen) and COS7 cells were cultured in Dulbecco's modified Eagle's medium (Sigma D5796) supplemented with 10% fetal bovine serum and antibiotic antimycotic solution (Sigma

A5955). Cells were transfected with plasmid DNAs by using Polyethylenimine "Max" (Polysciences) as described previously (Boussif et al. 1995). For inhibition of glycosylation of newly synthesized proteins, the medium was replaced 8 h after transfection with fresh medium containing tunicamycin (5 μg/ml). If necessary, 50 μg/ml cycloheximide, 50 nM concanamycin A, 20 μM MG132, or 5 μg/ml brefeldin A was used to prevent protein synthesis, lysosomal degradation, proteasomal degradation, or protein trafficking between the endoplasmic reticulum and Golgi apparatus, respectively. The cells were analyzed 24–36 h after transfection.

Immunoprecipitation and western blotting

Mouse tissues or cultured cells were lysed with buffer containing 50 mM Tris-Cl (pH 7.4), 150 mM NaCl, 2 mM EDTA, 2 mM phenylmethylsulfonyl fluoride, 2 mM Na_3VO_4, 20 mM NaF, and 1% Triton X-100. The lysates were separated by centrifugation for 20 min. For immunoprecipitation, the lysates were incubated with anti-FLAG, anti-GFP, or anti-SAMT1 at 4°C for 12–16 h and then with protein G-sepharose or protein A-sepharose beads for 2 h with gentle agitation. The immunoprecipitates were washed 4 times with lysis buffer and suspended with sample buffer. For the deglycosylation assay, the immunoprecipitates were denatured, incubated with peptide:*N*-glycosidase F (PNGase F; NEB) at 37°C for 1 h, and suspended with an equal volume of 2× sample buffer. The proteins were separated by SDS-PAGE, transferred onto a polyvinylidene difluoride membrane, and detected by western blotting. To detect the signal of immunoprecipitated SAMT1, Clean-Blot IP Detection Reagent (PIERCE) was used as a secondary antibody, if necessary, to avoid masking by immunoglobulin light chain bands.

Immunohistochemistry

Testes from ICR mice were collected, fixed in Bouin's solution, embedded in paraffin, and cut into 4-μm-thick sections. Sections were mounted on poly-L-lysine-coated glass slides, deparaffinized, rehydrated, and then incubated in 10 mM citrate buffer (pH 9.0) at 80°C for 30 min. For peroxidase staining, sections were treated with 3% H_2O_2 in PBS to block endogenous peroxidase activity. The sections were then blocked for 1 h with 10% goat serum in PBS, followed by incubation with primary antibody for 1 h. After being washed with PBS, the sections were incubated with HRP-conjugated goat anti-rabbit IgG antibody. Signals were visualized with diaminobenzidine, and tissue sections were counterstained with Mayer hematoxylin. For immunofluorescence analysis, the sections were processed similarly, and Alexa Fluor 488- or Alexa Fluor 568-conjugated secondary antibodies (Molecular Probes, dilution 1:500) were used to visualize the signals. Dilutions of primary antibody were as follows: rabbit anti-SMAT1 antibody, 3 μg/ml; rat anti-MARCH11 antibody, 1:1000; and mouse anti-GM130 antibody, 0.5 μg/ml. When necessary, DAPI and Alexa 488-conjugated lectin PNA (Molecular Probes) were used to stain the nuclei and acrosomes, respectively. The images were captured with a BX50 microscope (OLYMPUS) equipped with a DP50 CCD camera (OLYMPUS).

Confocal microscopic analysis

Seminiferous tubules were placed in microtubes and cut into small pieces in PBS. The cells were

mechanically dissociated by vigorous pipetting, and the cell suspension was filtered with a 70-μm nylon mesh to remove the debris, washed twice in minimum essential medium (Sigma), and placed on glass coverslips coated with poly-L-lysine. After incubation in a CO_2 incubator for 30 min, the cells were fixed with ice-cold methanol, permeabilized with 0.2% Triton X-100/PBS, and blocked with 5% skim milk/PBS for 1 h. Immunostaining of the cells was performed as described above, but Alexa Fluor 633-conjugated goat anti-rabbit IgG (Invitrogen) was used to detect SAMT1. For staining fucose-containing glycoproteins, the cells were incubated with 10 μg/ml biotin-labeled ALL (Vector Laboratories) in PBS for 90 min, and the signals were visualized with DyLight-488 conjugated streptavidin (KPL). COS7 cells grown on coverslips were also fixed and stained similarly. The images were scanned with a Leica TCL SL confocal microscope.

Results

Identification and mRNA expression of Samt *family genes*

To detect spermatogenesis-associated membrane proteins in mice, we identified 53 candidate genes by using in silico analysis, microarray data, as well as a transmembrane domain prediction tool. One of the genes, *4921511M17Rik/Gm15144*, was recently identified as one of the X-linked multicopy testis genes expressed in postmeiotic germ cells (Mueller et al. 2008). Hence, we named it *Samt1* (*spermatogenesis-associated multicopy transmembrane protein 1*, GenBank accession no. NM_030036). We also found 3 other related genes through BLAST search and named them *Samt2* (NM_001037167), *Samt3*

(NM_028554), and *Samt4* (NM_029199). All 4 *Samt* genes encode putative proteins that are predicted to have 4 transmembrane domains. However, they do not have any known functional domain. The family members show 47–62% homology at the protein level (Fig. 1a). Reverse transcriptase-PCR (RT-PCR) analysis showed that the *Samt* genes were specifically expressed in the testis (Fig. 1b). The expression of *Samt1–Samt4* mRNAs in mouse testis was detected 25–30 days after birth and increased gradually up to 45 days (Fig. 1c). In addition, their expression was not detected in W/W^v mouse testes (Fig. 1d), which lack germ cells (Russell 1979). These results suggested that *Samt1–Samt4* mRNAs were specifically expressed in haploid germ cells. Although 3 bands were consistently detected for *Samt4*, sequence analysis revealed that the 2 faster-migrating bands were splice variants of *Samt4*.

Expression and posttranslational modification of SAMT1

Among the SAMT family proteins, we mainly focused on SAMT1 because it was the only SAMT protein identified in the initial screening. To explore the expression of SAMT1, we developed an affinity-purified anti-SAMT1 antibody. This antibody specifically recognized SAMT1 and did not show cross-reactivity with other SAMT family proteins (data not shown). Immunoprecipitation and western blot analysis of various mouse tissue lysates showed that SAMT1 expression was restricted to the testis (Fig. 2a, left panel), which was consistent with the mRNA expression pattern. No signal was detected when control rabbit IgG was used for immunoprecipitation (Fig. 2a, right panel). The molecular mass of the major SAMT1 band was estimated at ~34 kDa and was slightly higher than the mass calculated from the amino

acid composition. We speculated that SAMT1 was modified after translation, and examined the possibility that it was glycosylated. Treatment with PNGase F decreased the molecular mass to an estimated value of ~27 kDa and resulted in the disappearance of the additional faint band, indicating that SAMT1 was *N*-linked glycosylated (Fig. 2b). SAMT2, SAMT3, and SAMT4 were also found to be glycosylated to varying degrees when expressed in 293F cells (Fig. 2c). When cells were treated with tunicamycin 8 h after transfection to inhibit the glycosylation of newly synthesized proteins, the expression of all SAMT family proteins was markedly impaired (Fig. 2d). These results indicate that *N*-linked glycosylation is essential for the expression of SAMT family proteins.

Cellular and intracellular localization of SAMT1

We then examined the expression and cellular localization of SAMT1 in mouse testis during postnatal development. Immunohistochemical analysis revealed that SAMT1 expression was first detected 25 days after birth as a signal in the inner layer of the seminiferous tubes where the spermatids were localized. No signal was detected in spermatogonia, spermatocytes, Sertoli cells, or Leydig cells (Fig. 3). As spermatogenesis proceeded, the number of SAMT1-expressing cells increased, whereas mature sperm cells in the epididymis did not show staining. These results indicate that SAMT1 was expressed in the spermatids in a stage-specific manner during spermiogenesis.

Spermiogenesis is divided into 4 phases: the Golgi, cap, acrosome, and maturation phases. Each phase can be morphologically distinguished by the shape of the acrosome and nuclei. To identify the phase

expressing SAMT1, immunofluorescence staining was performed using PNA-lectin, DAPI, and anti-SAMT1 antibody. As shown in Figure 4a, SAMT1 signal was absent in the Golgi phase but clearly detectable in the cap phase of spermiogenesis. During this phase, SAMT1 exhibited a punctate localization pattern and was often observed adjacent to the nucleus and sometimes to the acrosome. SAMT1 signal was still detectable in early acrosome phase spermatids, but the localization appeared to have moved to the posterior of the cell. In the late acrosome phase, the signal was less frequently observed and eventually disappeared during the maturation phase. To define the intracellular localization of SAMT1, the sections were double immunostained with anti-GM130 antibody, a Golgi apparatus marker. As previously reported, the Golgi apparatus is crescent shaped and located near the nucleus in the cap-phase spermatid (Clermont et al. 1993). Intriguingly, some of the punctate regions of SAMT1 localized to the concave portion of the Golgi apparatus (Fig. 4b, arrow). This region corresponded to the "Golgi medulla," which is rich in vesicles from the TGN (Clermont et al. 1993). The association between the Golgi apparatus and SAMT1 was not observed in later phases. The expression and staining patterns of SAMT1 in spermatids closely resembled those of MARCH11, which is known to localize to the TGN vesicles and MVBs (Morokuma et al. 2007). Using immunofluorescence staining, we confirmed that MARCH11 was expressed in mouse spermatids, and found SAMT1 and MARCH11 to be concurrently expressed (Fig. 4c). Furthermore, confocal microscopic analysis showed that SAMT1 co-localized with MARCH11 in round spermatids (Fig. 5). SAMT1 also co-localized with fucose-containing glycoproteins labeled by AAL lectin, another marker of TGN vesicles and MVBs (Martinez-Menarguez et al. 1996a; Tang et al. 1982; Morokuma et al. 2007), and with LAMP2, a late endosome/lysosome marker

(Granger et al. 1990) (Fig. 5). These results clearly indicate that SAMT1 localizes to the TGN vesicles and MVBs or late endosomes/lysosomes in spermatids.

Localization and oligomer formation of SAMT family proteins

We next examined the intracellular localization of other SAMT family proteins by using COS7 cells. Non-tagged SAMT1 and FLAG-tagged SAMT2, SAMT3, and SAMT4 were expressed, and their localization was analyzed by confocal microscopy. SAMT1 was observed near the nucleus and in spotted structures that were presumed to be the Golgi apparatus and intracellular vesicles. SAMT2, SAMT3, and SAMT4 also showed similar intracellular localization, and their immunofluorescence signals completely overlapped with those of SAMT1 (Fig. 6a). In addition, when SAMT family proteins were co-expressed with MARCH11, all SAMT proteins co-localized with MARCH11 (Fig. 6b). These results suggest that SAMT2–SAMT4 as well as SAMT1 were localized to the TGN and MVBs in mouse spermatids. In addition, the above results raised the possibility that SAMT1 could oligomerize with other SAMT proteins and with itself. To assess this possibility, GFP-tagged SAMT1 (SAMT1-GFP) and FLAG-tagged SAMT1–SAMT4 were expressed in 293F cells, and oligomerization was analyzed with immunoprecipitation followed by western blotting. To address the masking of the SAMT1-GFP signal by IgG heavy chain, the immunoprecipitates were treated with PNGase F. SAMT1-GFP co-immunoprecipitated with all the SAMT family proteins, whereas GFP alone did not bind (Fig. 6c and d). These results suggest that SAMT1 can oligomerize and function as a part of a protein complex.

Ubiquitination and degradation of SAMT1 by MARCH11

The co-localization of SAMT family proteins and MARCH11 suggested that some functional relation exists between these proteins. We assumed that SAMT might be a substrate of MARCH11 and examined the ubiquitination of SAMT family proteins using 293F cells. 293F cells were chosen for ease of use given the challenges encountered in the purification and gene transfection of round spermatids. FLAG-tagged SAMT1–SAMT4, MARCH11, and ubiqutin were expressed, and ubiquitination was monitored by immunoprecipitation and western blotting. To prevent the lysosomal degradation of SAMT1, concanamycin A, a specific inhibitor of vacuolar type H^+-ATPase, was used (see below). As expected, we observed increased ubiquitination of all SAMT proteins when co-expressed with MARCH11 (Fig. 7a). If ubiquitination induced by MARCH11 acts as a sorting signal for SAMT1 into MVB, SAMT1 is predicted to be rapidly degraded in the presence of MARCH11. Thus, we investigated this possibility using cycloheximide chase assay and found that MARCH11 significantly reduced the half-life of SAMT1 (Fig. 7b). Interestingly, although 3 bands of SAMT1 were usually observed when SAMT1 was expressed in 293F cells (Figs. 2 and 7), only the most slowly migrating form of SAMT1 remained after inhibition of protein synthesis in the absence of MARCH11 (Fig. 7b). In contrast, the amount of the slow-migrating form of SAMT1 is much lower in the presence of MARCH11, whereas 2 faster migrating bands were detected at similar amounts as in the absence of MARCH11 (Fig. 7b). These results suggested that SAMT1 was glycosylated in a stepwise manner during endoplasmic reticulum (ER)–Golgi apparatus trafficking, and that fully glycosylated SAMT1 (most slowly

migrating band) that left the TGN was more rapidly delivered to lysosomes and degraded when MARCH11 was overexpressed. In fact, treatment with brefeldin A, an inhibitor of protein trafficking from ER to Golgi, caused a shift in the mobility of SAMT1 (Fig. 7c), and MARCH11-induced rapid degradation of SAMT1 was inhibited by concanamycin A, but not by the proteasome inhibitor MG132 (Fig. 7d). Furthermore, we found that the MARCH11-induced degradation of SAMT1 required the ubiquitin ligase activity of MARCH11, and that the degradation of other SAMT proteins was also enhanced by MARCH11 (Fig. 7e).

Effect of C-terminal deletion on ubiquitination and intracellular localization of SAMT1

Finally, we tried to identify the region for ubiquitination in SAMT1. The N-terminal, second loop, and C-terminal regions of SAMT1 are predicted to be on the cytoplasmic side where the RING-finger domain of MARCH11 is positioned. Because the C-terminal tail of SAMT1 contains a relatively high number of lysine residues, we examined whether the region was a major site for ubiquitination by using a deletion mutant that lacks 19 amino acids from the C-terminus. Results showed that the ubiquitination level of the mutant was significantly lower than that of the wild type (Fig. 8a). Then, we examined the effect of the deletion of the C-terminus region on the intracellular localization of the protein. Wild-type SAMT1 was observed near the nucleus and in spotted structures as previously described (Fig. 8b). In contrast, the deletion mutant of SAMT1 showed diffuse and uniform localization in the cytoplasm (Fig. 8b). These results suggest that the C-terminal region is indispensable for the ubiquitination and proper localization of SAMT1.

Discussion

The *Samt1* gene was first identified by genomic data mining as one of the X-linked multicopy testis genes expressed in postmeiotic germ cells (Mueller et al. 2008); however, a functional analysis of the gene has not been performed. In this study, we also identified *Samt1* as a spermatogenesis-associated transmembrane protein gene, and we characterized the expression and the intracellular localization and posttranslational modification of SAMT1 in mice.

Samt is a highly related, small multigene family consisting of 4 members. They encode putative, 4-transmembrane proteins with no known homology to other proteins. RT-PCR analysis showed that the expression profiles of *Samt* family genes during postnatal testis development were very similar. In addition, their expression was not detected in W/W^v mouse testes, which lack germ cells, suggesting that all SAMT family proteins are specifically expressed in spermatids. Furthermore, SAMT family proteins are *N*-linked glycosylated proteins that show an identical intracellular localization when expressed in COS7 cells. Taken together, these results suggest that the SAMT family proteins have similar molecular characteristics and may play similar roles in spermatogenesis.

In this study, we found that SAMT1 localized to the TGN and MVBs but not to the acrosome. SAMT1 also appeared to be localized to late endosomes or lysosomes. These results demonstrate that SAMT1 is selectively transported from the TGN to MVBs and finally to lysosomes. Ubiquitination functions as a signal for sorting transmembrane proteins into MVBs. For example, upon endocytosis, plasma membrane

proteins such as activated growth factor receptor are labeled with ubiquitin and captured by the endosomal sorting complex for transport (ESCRT) machinery. The ESCRT machinery consists of 4 complexes (i.e., Escrt-0, Escrt-I, Escrt-II, and Escrt-III). These complexes sequentially and cooperatively act in the recognition and sorting of ubiquitinated cargo and in the formation of intraluminal vesicles (Piper and Katzmann 2007; Raiborg and Stenmark 2009). In addition to endocytosis, ubiquitination-mediated vesicle trafficking from the TGN to the endosome has been demonstrated in yeast. Ubiquitination of Gap1 by the Rsp5p E3 ligase complex is required for the sorting of Gap1 from the TGN into the vacuole, a lysosome-like organelle in yeast (Helliwell et al. 2001; Lauwers et al. 2009). Similarly, carboxypeptidase S requires ubiquitination for proper sorting into MVBs (Reggiori and Pelham 2002). In contrast to yeast, in mammalian cells, little is known about such cargo proteins that are transported from the TGN to MVBs by ubiquitin-mediated sorting. In this study, we found that MARCH11 increased the ubiquitination of SAMT1. MARCH11 also enhanced the lysosomal delivery and degradation of SAMT1 dependent on its ligase activity. These results suggest that SAMT1 is a substrate of MARCH11, and that MARCH11 is involved in the selective sorting of SAMT1 into MVBs and its subsequent degradation in lysosomes. On the other hand, we could not demonstrate whether MARCH11 is essential for the ubiquitination and degradation of SAMT1 in spermatids. We performed a knockdown experiment for mouse spermatids, but the attempt failed owing to technical reasons, including low transfection efficiency and the difficulty of purification and biochemical analysis in spermatids. In addition, since it has been shown that other members of the *March* family are expressed in rat testis and some MARCH proteins seem to share common substrates (Morokuma et al. 2007;

Nathan and Lehner 2009), the essential role of MARCH11 in the ubiquitination of SAMT1 in mouse spermatids needs to be carefully elucidated.

An additional finding of this study was that the C-terminal region of SAMT1 was indispensable for the ubiquitination and proper localization of SAMT1. MARCH11 may ubiquitinate the lysine residue(s) in the C-terminal region of SAMT1, and the ubiquitination acts as a sorting signal for selective transport of SAMT1 into MVBs. However, the mechanism of transport of ubiquitinated SAMT1 is yet unknown. It has been reported that GGA (Golgi-associated, γ-adaptin homologous, ARF-interacting proteins) family proteins could bind to ubiquitin and act as sorting receptors (Scott et al. 2004). GGAs localize to the TGN and are involved in protein transport from the TGN to the endosomal–lysosomal system through incorporation of proteins into clathrin-coated vesicles. Although their expression is yet to be investigated in spermatids, GGA proteins are candidate transporters of ubiquitinated SAMT1 from the TGN to MVBs.

SAMT1 was found to be specifically expressed during the cap and acrosome phases but not during the Golgi and maturation phases of spermiogenesis. However, previous electron microscopic analysis has revealed that MVBs are already present in spermatocytes (Haraguchi et al. 2004). Therefore, SAMT1 may play a dispensable role in the formation of MVB. A possible function of SAMT1 is the mediation of protein transport from the TGN to MVBs. SAMT1 interacts with some specific protein in the TGN, and this complex is incorporated into an endosomal vesicle and transported to MVB. With regard to this possibility, we found that SAMT protein was able to form oligomer complexes, suggesting its potential role as a protein interactor. Another possibility is that SAMT1 regulates the formation of the intraluminal vesicles of MVBs similar to the

tetraspanin superfamily proteins such as CD63. Tetraspanins are a major component of MVBs and form complexes with various proteins and lipids called tetraspanin-enriched microdomains, which are implicated in the generation of membrane curvature, budding, and fission (Huttner and Zimmerberg 2001; Ikonen 2001; Hemler 2003), presumably through association with the cytoskeletal machinery and cholesterol (Charrin et al. 2003; Silvie et al. 2006; Hemler 2003). Deformation of the membrane could be induced not only by tetraspanins but also by other 4-transmembrane proteins such as Peripherin/rds (Wrigley et al. 2000). Interestingly, tetraspanins, Peripherin/rds, and SAMT1 share structural and biochemical similarities (i.e., 4 transmembrane spans, oligomerization, and modification through glycosylation) (Cannon and Cresswell 2001; Wrigley et al. 2000; Kovalenko et al. 2004). In any case, SAMT1 is hypothesized to act as a regulator in protein transport and/or degradation during specific phases of spermatogenesis, and its function may contribute to the normal morphogenesis of mouse sperms.

Recent studies clearly indicate that proper membrane trafficking is important for spermatogenesis. In post-Golgi transport, it has been shown that GOPC plays an essential role in acrosome and nuclear formation and in normal arrangement of the mitochondria (Yao et al. 2002). Similarly, deficiency of protein interacting with C kinase 1 (PICK1), which is highly expressed in round spermatids and is involved in vesicle trafficking from the Golgi apparatus to the acrosome, causes globozoospermia and infertility in male mice (Xiao et al. 2009). Further, Rainey et al. (2010) showed that EHD1, a regulator of endocytic recycling/sorting, was essential for normal sperm morphogenesis in mice (Rainey et al. 2010). In this study, we identified SAMT1 as a novel, TGN- and MVB-localized protein that may function in vesicle trafficking and/or protein

degradation. Although the existence of MVBs in male germ cells has been described as early as in 1960 (Mollenhauer and Zebrun 1960), their function is still largely unknown. Our findings could provide an insight into their molecular functions in spermatogenesis.

Acknowledgement

This work was supported by United Graduate School of Agricultural Science (Gifu University) Education and Research Activation Grants.

References

Boussif O, Lezoualc'h F, Zanta MA, Mergny MD, Scherman D, Demeneix B, Behr JP (1995) A versatile vector for gene and oligonucleotide transfer into cells in culture and in vivo: polyethylenimine. Proc Natl Acad Sci U S A 92 (16):7297-7301

Braun RE (1998) Post-transcriptional control of gene expression during spermatogenesis. Semin Cell Dev Biol 9 (4):483-489

Cannon KS, Cresswell P (2001) Quality control of transmembrane domain assembly in the tetraspanin CD82. Embo J 20 (10):2443-2453

Charrin S, Manie S, Thiele C, Billard M, Gerlier D, Boucheix C, Rubinstein E (2003) A physical and functional link between cholesterol and tetraspanins. Eur J Immunol 33 (9):2479-2489

Clermont Y (1972) Kinetics of spermatogenesis in mammals: seminiferous epithelium cycle and spermatogonial renewal. Physiol Rev 52 (1):198-236

Clermont Y, Oko R, Hermo L (1993) Cell biology of mammalian spermiogenesis. In: Desjardins C, Ewing LL (eds), Cell and Molecular Biology of the Testis, Oxford University Press, New York, pp332-376

Clermont Y, Tang XM (1985) Glycoprotein synthesis in the Golgi apparatus of spermatids during spermiogenesis of the rat. Anat Rec 213 (1):33-43

Eddy EM (2002) Male germ cell gene expression. Recent Prog Horm Res 57:103-128

Granger BL, Green SA, Gabel CA, Howe CL, Mellman I, Helenius A (1990) Characterization and cloning of lgp110, a lysosomal membrane glycoprotein from mouse and rat cells. J Biol Chem 265 (20):12036-12043

Griffiths G, Warren G, Stuhlfauth I, Jockusch BM (1981) The role of clathrin-coated vesicles in acrosome formation. Eur J Cell Biol 26 (1):52-60

Haraguchi CM, Mabuchi T, Hirata S, Shoda T, Hoshi K, Akasaki K, Yokota S (2005) Chromatoid bodies: aggresome-like characteristics and degradation sites for organelles of spermiogenic cells. J Histochem Cytochem 53 (4):455-465

Haraguchi CM, Mabuchi T, Hirata S, Shoda T, Hoshi K, Yokota S (2004) Ubiquitin signals in the developing acrosome during spermatogenesis of rat testis: an immunoelectron microscopic study. J Histochem Cytochem 52 (11):1393-1403

Helliwell SB, Losko S, Kaiser CA (2001) Components of a ubiquitin ligase complex specify polyubiquitination and intracellular trafficking of the general amino acid permease. J Cell Biol 153 (4):649-662

Hemler ME (2003) Tetraspanin proteins mediate cellular penetration, invasion, and fusion events and define a novel type of membrane microdomain. Annu Rev Cell Dev Biol

19:397-422

Hermo L, Pelletier RM, Cyr DG, Smith CE (2010) Surfing the wave, cycle, life history, and genes/proteins expressed by testicular germ cells. Part 2: changes in spermatid organelles associated with development of spermatozoa. Microsc Res Tech 73 (4):279-319

Huttner WB, Zimmerberg J (2001) Implications of lipid microdomains for membrane curvature, budding and fission. Curr Opin Cell Biol 13 (4):478-484

Ikonen E (2001) Roles of lipid rafts in membrane transport. Curr Opin Cell Biol 13 (4):470-477

Inoue N, Ikawa M, Isotani A, Okabe M (2005) The immunoglobulin superfamily protein Izumo is required for sperm to fuse with eggs. Nature 434 (7030):234-238

Kovalenko OV, Yang X, Kolesnikova TV, Hemler ME (2004) Evidence for specific tetraspanin homodimers: inhibition of palmitoylation makes cysteine residues available for cross-linking. Biochem J 377 (Pt 2):407-417

Lauwers E, Jacob C, Andre B (2009) K63-linked ubiquitin chains as a specific signal for protein sorting into the multivesicular body pathway. J Cell Biol 185 (3):493-502

Martinez-Menarguez JA, Geuze HJ, Ballesta J (1996a) Evidence for a nonlysosomal origin of the acrosome. J Histochem Cytochem 44 (4):313-320

Martinez-Menarguez JA, Geuze HJ, Ballesta J (1996b) Identification of two types of beta-COP vesicles in the Golgi complex of rat spermatids. Eur J Cell Biol 71 (2):137-143

Mollenhauer HH, Zebrun W (1960) Permanganate fixation of the Golgi complex and other cytoplasmic structures of mammalian tests. J Biophys Biochem Cytol 8:761-775

Moreno RD, Ramalho-Santos J, Chan EK, Wessel GM, Schatten G (2000) The Golgi apparatus segregates from the lysosomal/acrosomal vesicle during rhesus spermiogenesis: structural alterations. Dev Biol 219 (2):334-349

Morokuma Y, Nakamura N, Kato A, Notoya M, Yamamoto Y, Sakai Y, Fukuda H, Yamashina S, Hirata Y, Hirose S (2007) MARCH-XI, a novel transmembrane ubiquitin ligase implicated in ubiquitin-dependent protein sorting in developing spermatids. J Biol Chem 282 (34):24806-24815

Mueller JL, Mahadevaiah SK, Park PJ, Warburton PE, Page DC, Turner JM (2008) The mouse X chromosome is enriched for multicopy testis genes showing postmeiotic expression. Nat Genet 40 (6):794-799

Nathan JA, Lehner PJ (2009) The trafficking and regulation of membrane receptors by the RING-CH ubiquitin E3 ligases. Exp Cell Res 315 (9):1593-1600

Parvinen M (2005) The chromatoid body in spermatogenesis. Int J Androl 28 (4):189-201

Piper RC, Katzmann DJ (2007) Biogenesis and function of multivesicular bodies. Annu Rev Cell Dev Biol 23:519-547

Raiborg C, Stenmark H (2009) The ESCRT machinery in endosomal sorting of ubiquitylated membrane proteins. Nature 458 (7237):445-452

Rainey MA, George M, Ying G, Akakura R, Burgess DJ, Siefker E, Bargar T, Doglio L, Crawford SE, Todd GL, Govindarajan V, Hess RA, Band V, Naramura M, Band H (2010) The endocytic recycling regulator EHD1 is essential for spermatogenesis and male fertility in mice. BMC Dev Biol 10:37

Ramalho-Santos J, Moreno RD (2001) Targeting and fusion proteins during mammalian spermiogenesis. Biol Res 34 (2):147-152

Ramalho-Santos J, Moreno RD, Wessel GM, Chan EK, Schatten G (2001) Membrane trafficking machinery components associated with the mammalian acrosome during spermiogenesis. Exp Cell Res 267 (1):45-60

Ramalho-Santos J, Schatten G, Moreno RD (2002) Control of membrane fusion during spermiogenesis and the acrosome reaction. Biol Reprod 67 (4):1043-1051

Reggiori F, Pelham HR (2002) A transmembrane ubiquitin ligase required to sort membrane proteins into multivesicular bodies. Nat Cell Biol 4 (2):117-123

Russell ES (1979) Hereditary anemias of the mouse: a review for geneticists. Adv Genet 20:357-459

Schultz N, Hamra FK, Garbers DL (2003) A multitude of genes expressed solely in meiotic or postmeiotic spermatogenic cells offers a myriad of contraceptive targets. Proc Natl Acad Sci U S A 100 (21):12201-12206

Scott PM, Bilodeau PS, Zhdankina O, Winistorfer SC, Hauglund MJ, Allaman MM, Kearney WR, Robertson AD, Boman AL, Piper RC (2004) GGA proteins bind ubiquitin to facilitate sorting at the trans-Golgi network. Nat Cell Biol 6 (3):252-259

Shima JE, McLean DJ, McCarrey JR, Griswold MD (2004) The murine testicular transcriptome: characterizing gene expression in the testis during the progression of spermatogenesis. Biol Reprod 71 (1):319-330

Silvie O, Charrin S, Billard M, Franetich JF, Clark KL, van Gemert GJ, Sauerwein RW, Dautry F, Boucheix C, Mazier D, Rubinstein E (2006) Cholesterol contributes to the organization of tetraspanin-enriched microdomains and to CD81-dependent infection by malaria sporozoites. J Cell Sci 119 (Pt 10):1992-2002

Tanaka H, Baba T (2005) Gene expression in spermiogenesis. Cell Mol Life Sci 62 (3):344-354

Tang XM, Lalli MF, Clermont Y (1982) A cytochemical study of the Golgi apparatus of the spermatid during spermiogenesis in the rat. Am J Anat 163 (4):283-294

Ventela S, Toppari J, Parvinen M (2003) Intercellular organelle traffic through cytoplasmic bridges in early spermatids of the rat: mechanisms of haploid gene product sharing. Mol Biol Cell 14 (7):2768-2780

Wolfsberg TG, Straight PD, Gerena RL, Huovila AP, Primakoff P, Myles DG, White JM (1995) ADAM, a widely distributed and developmentally regulated gene family encoding membrane proteins with a disintegrin and metalloprotease domain. Dev Biol 169 (1):378-383

Wrigley JD, Ahmed T, Nevett CL, Findlay JB (2000) Peripherin/rds influences membrane vesicle morphology. Implications for retinopathies. J Biol Chem 275 (18):13191-13194

Xiao N, Kam C, Shen C, Jin W, Wang J, Lee KM, Jiang L, Xia J (2009) PICK1 deficiency causes male infertility in mice by disrupting acrosome formation. J Clin Invest 119 (4):802-812

Yao R, Ito C, Natsume Y, Sugitani Y, Yamanaka H, Kuretake S, Yanagida K, Sato A, Toshimori K, Noda T (2002) Lack of acrosome formation in mice lacking a Golgi protein, GOPC. Proc Natl Acad Sci U S A 99 (17):11211-11216

Yoshinaga K, Toshimori K (2003) Organization and modifications of sperm acrosomal molecules during spermatogenesis and epididymal maturation. Microsc Res Tech 61 (1):39-45

Figure captions

Fig. 1 Isolation and mRNA expression of *Samt* family genes.

a Multiple sequence alignment of the deduced amino acid sequences of mouse *Samt* family genes. Letters in bold represent the putative transmembrane regions predicted by the TMHMM server program. The underlined regions were used as antigen. **b** RT-PCR analysis of *Samt* family gene expression in various tissues. *Gapdh* was used as an internal control. **c** Changes in the expression levels of *Samt* family genes during postnatal testis development. The numbers indicate the days after birth. **d** mRNA expression of *Samt* family genes in wild-type and W/W^v mouse testis

Fig. 2 Testicular expression and *N*-linked glycosylation of SAMT1.

a Expression of SAMT1 in various mouse tissues as observed using anti-SAMT1 antibody (left panel). Immunoprecipitates with control normal rabbit IgG (Cont) or anti-SAMT1 antibody from mature mouse testis extracts (right panel). The same filter was reprobed with anti-rabbit IgG to monitor that an equal amount of antibody was used for immunoprecipitation in each lane (bottom panel). **b** Glycosylation of SAMT1. Immunoprecipitated SAMT1 was treated with or without PNGase F for 1 h. **c** Glycosylation of other SAMT family proteins. SAMT1–SAMT4 expression vectors were introduced into 293F cells, and glycosylation was analyzed as in b. Asterisks indicate immunoglobulin heavy chain and light chain. **d** Effect of glycosylation inhibition on the expression of SAMT family proteins. 293F cells expressing the FLAG-tagged SAMT1–SAMT4 vectors were treated with 5 μg/ml tunicamycin (TM)

Fig. 3 Immunohistochemical localization of SAMT1 during postnatal testis development. SAMT1 signal is visualized by the brown coloration. The numbers indicate the days after birth. Bar, 20 μm

Fig. 4 Stage-specific expression and intracellular localization of SAMT1 in mouse spermatids.

a Triple immunofluorescence staining of the acrosomes (green), nuclei (blue), and SAMT1 (red) in spermatids at various stages of spermiogenesis. G, Golgi phase; C, cap phase; EA, early acrosome phase; LA, late acrosome phase; M, maturation phase. **b** Immunofluorescence staining of GM130 (green), SAMT1 (red), and nuclei (blue). Arrows point to the concave region of the Golgi apparatus, and arrowheads point to SAMT1 not associated with the Golgi apparatus. **c** Immunofluorescence staining of MARCH11 (green), SAMT1 (red), and nuclei (blue). Sc, spermatocytes. Bar, 10 μm

Fig. 5 Immunofluorescence confocal microscopic analysis of SAMT1 in mouse round spermatids.

Mouse round spermatids isolated from seminiferous tubule were immunostained with rabbit anti-SAMT1 antibody (a–c; red) and rat anti-MARCH11 antibody (a; green), AAL-lectin (b; green), or rat anti-LAMP2 antibody (c; green). Nuclei were stained with propidium iodide (a–c; blue). Immunofluorescence signals were detected by confocal microscopy and shown in pseudo-color. Bar, 10 μm

Fig. 6 Co-localization and oligomerization of SAMT family proteins.

a Non-tagged SAMT1 was co-expressed with FLAG-tagged SAMT2, SAMT3, and SAMT4 in COS7 cells, and their intracellular localization was monitored by immunofluorescence staining using anti-FLAG antibody (top panel) and anti-SAMT1 antibody (middle panel). The signals were detected with a confocal microscope. **b** FLAG-tagged SAMT1–SAMT4 were co-expressed with MARCH11, and their intracellular localization was monitored similarly. **c** GFP or SAMT1-GFP was expressed with SAMT1-FLAG in 293F cells, and the interaction was monitored by immunoprecipitation followed by western blotting with anti-GFP or anti-FLAG antibody. The combinations of expression vectors were as follows: lanes 1 and 4, empty vector only; lanes 2 and 5, GFP and Samt1-FLAG; lanes 3 and 6, SAMT1-GFP and SAMT1-FLAG. **d** GFP-SAMT1 was expressed with FLAG-tagged SAMT family proteins, and the interactions were monitored as in c

Fig. 7 Ubiquitination and lysosomal degradation of SAMT1 induced by MARCH11.

a FLAG-tagged SAMT1–SAMT4, MARCH11, and ubiquitin were expressed in 293F cells in the indicated combinations. After treatment with 50 nM concanamycin A for 8 h, cell lysates were collected, and ubiquitination of SAMT proteins was analyzed by immunoprecipitation and western blotting with anti-ubiquitin antibody, anti-FLAG antibody, or rabbit polyclonal anti-MARCH11 antibody. Asterisks indicate immunoglobulin heavy chain and light chain. WCL, whole cell lysate. **b** SAMT1-FLAG was expressed in 293F cells with or without MARCH11. After 24 h of transfection, 50 μg/ml cycloheximide was added to the culture, and cell lysates were collected 0, 1, 2, and 4 h after the treatment. The expression of SAMT1 and MARCH11 was monitored by immunoprecipitation and western blotting. β-Actin was used as a

Fig. 1

a

```
SAMT1  MDQLIVDTRSVIYRFINEKDCIYKLSGLLSSLAAFMLEVLIASILSWRLWEFDSNVVQFV 60
SAMT2  MDCYTLNTK----RFAG-LEWIFRVTGFICSLLSLGFGIILANSKYWRLWEFDNNVVQLV 55
SAMT3  MNFLTCDIQ----RFAVSKEYIFRLSGLICSLTAVVFEIILANSRCWRLWEFDDKTVQFV 56
SAMT4  MDLFTLDTQ----RFSKEKKSIFKLTGLFSSLSALVFEIAIASNQCWRLWEFEDDDVQFV 56
       *:    : :    **    . *::::*::.** :. : : :*.   ******:.. **:*

SAMT1  SFGLFEAYYPQQFNISGTLTKMLVYTPIDSTWNISTEFMYAQNLVVWAILMKPVVLVFCV 120
SAMT2  YIGLWEAYYHWEFNFSGTETIILVHSPVNSTWTISPEFQYARNLILLAMLIKPVVVIFSS 115
SAMT3  FFGLWEAYYHQVFNISGSTTRTLVHSPINSTWTISPEFHYAQTLIVWAILLKPVVLLFNA 116
SAMT4  SFGLWGAYYPKLFNISGTLVKMLVHNPIDSTWTISLEFQYAQNLILWAIFMKLVVLVFSV 116
        :**: ***   **:**: .  **:.*::***.** ** **:.*:: *:::* **::*

SAMT1  MAIKISCTKNPLVEMQIYCYKISALILSVSSMFTFVSVIWNHMVDFYGHTTLDFPSDFPV 180
SAMT2  AALRVSIIKASVPEIQIVCYKCSVLILILSSLCTIISVTWNHVVDLYGNTTLDFPPTFPV 175
SAMT3  MAVKIDYTNDSFVKGQMLLYKISASLLCISSLCTFVSVSWNHVVDLYGQTTLDFPPSFPV 176
SAMT4  IAFRISCMKDPFLMMQIYCYKFSTLVLGISSLFIFVAVSWNHMVDLYGQTTLDFPPKFPV 176
        *.::.  : ..   *:  ** *. :* :**:  ::* ***:**:**:******. ***

SAMT1  KKEALTSKHLTVVLPVGLLIATMSLFGVIMFLSEISDLKLKRPVKANDASKMGLLDA--- 237
SAMT2  KKEALIKKHNTHVFPMGLVTTTLSLFGVIMFLYEIRSLKVQKKLNAQHVSKQSDDRSINE 235
SAMT3  KKKDLKMKHYTAAFPIGVLTATMSLFGVIIFLFEMSSLDPQSEVEAQCASRLINQKT--- 233
SAMT4  QKEALKNKYVTAVFPVGILTATMSLFGGIMFLSEISYLKIQSQVEAKSVSKVALQEA--- 233
       :*: *  *: * .:*:*:: :*:**** *:** *:  *. :  ::*: .*:     :

SAMT1  ------------
SAMT2  HACVCQMCQETP 247
SAMT3  ------------
SAMT4  ------------
```

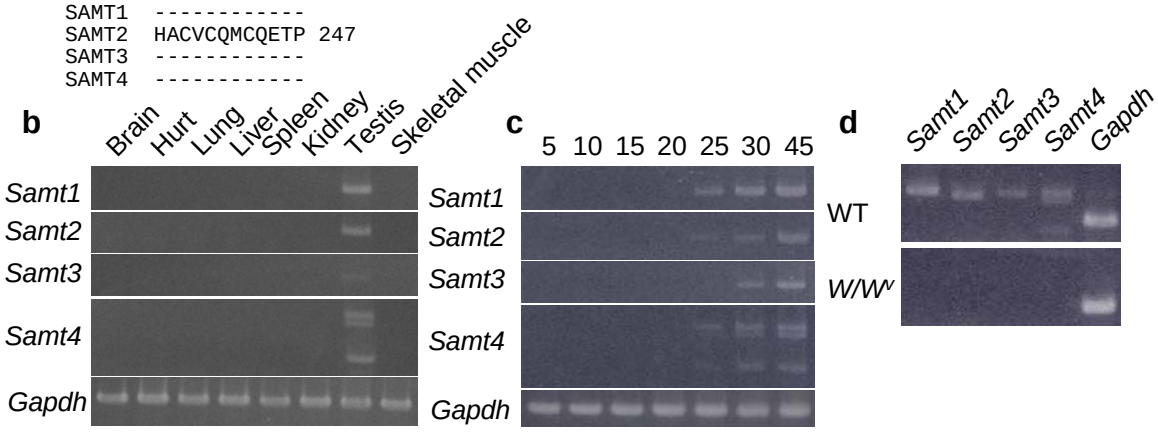

Fig. 2

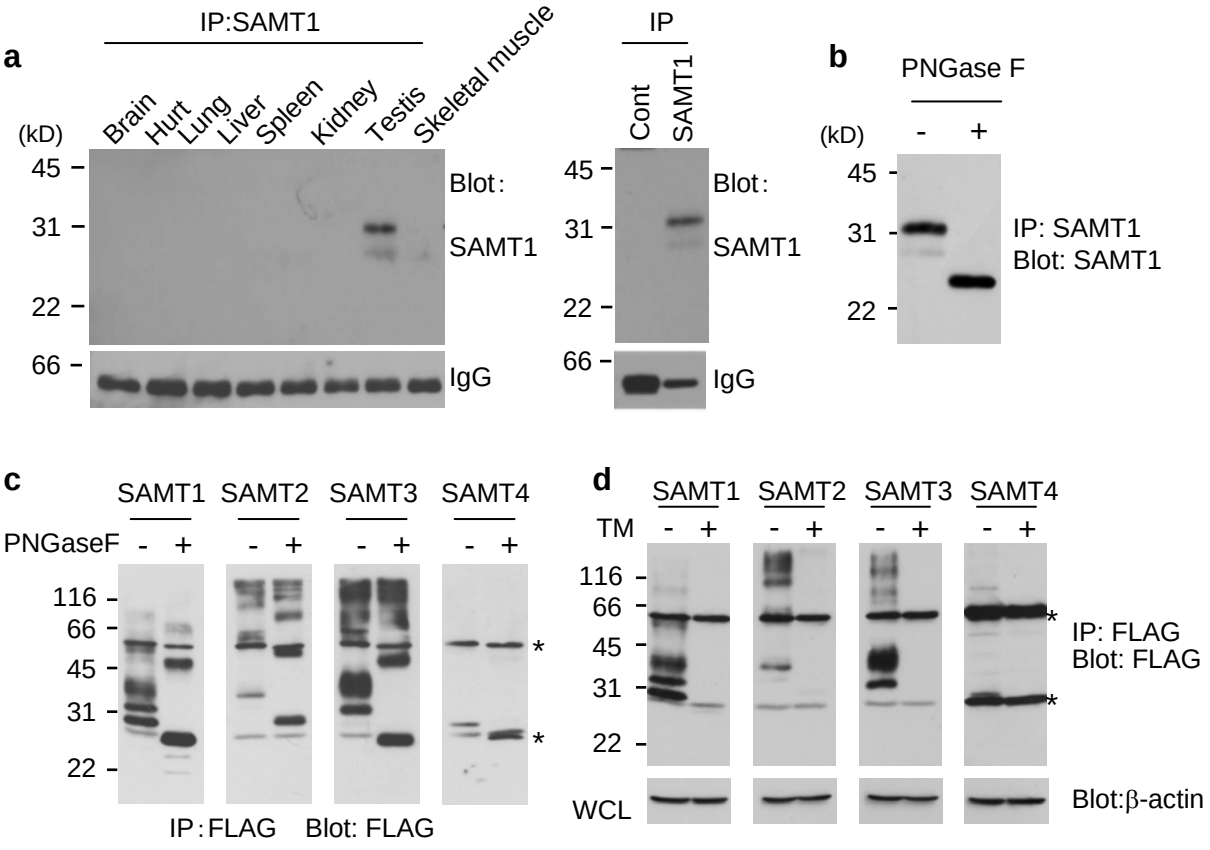
a
IP:SAMT1
Brain
Hurt
Lung
Liver
Spleen
Kidney
Testis
Skeletal muscle
(kD)
45
31
22
66
Blot:
SAMT1
IgG
IP
Cont
SAMT1
b
PNGase F
- +
IP: SAMT1
Blot: SAMT1
c
SAMT1 SAMT2 SAMT3 SAMT4
PNGaseF - + - + - + - +
116
66
45
31
22
*
IP: FLAG Blot: FLAG
d
SAMT1 SAMT2 SAMT3 SAMT4
TM - + - + - + - +
IP: FLAG
Blot: FLAG
WCL
Blot:β-actin

Fig. 3

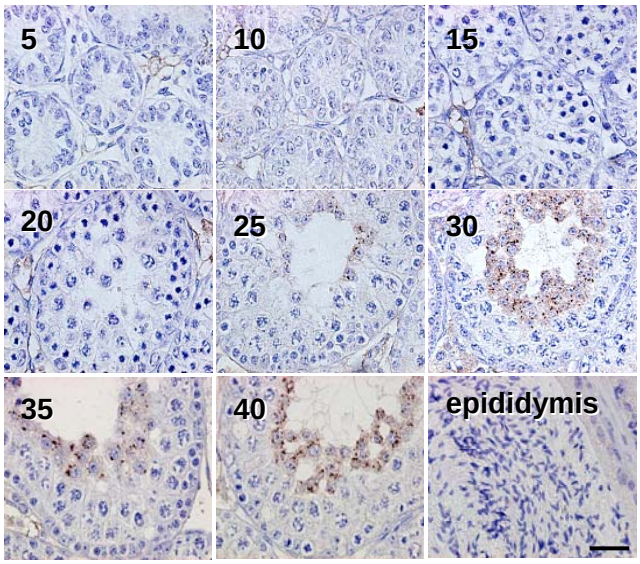

Fig. 4

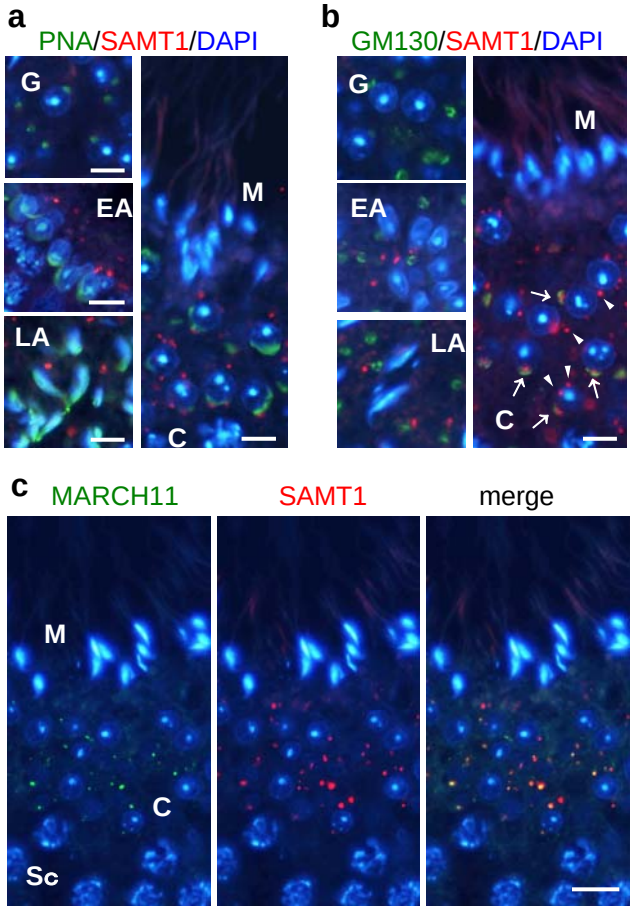
a
PNA/SAMT1/DAPI
G
EA
LA
M
C
b
GM130/SAMT1/DAPI
G
EA
LA
M
C
c
MARCH11
SAMT1
merge
M
C
Sc

Fig. 5

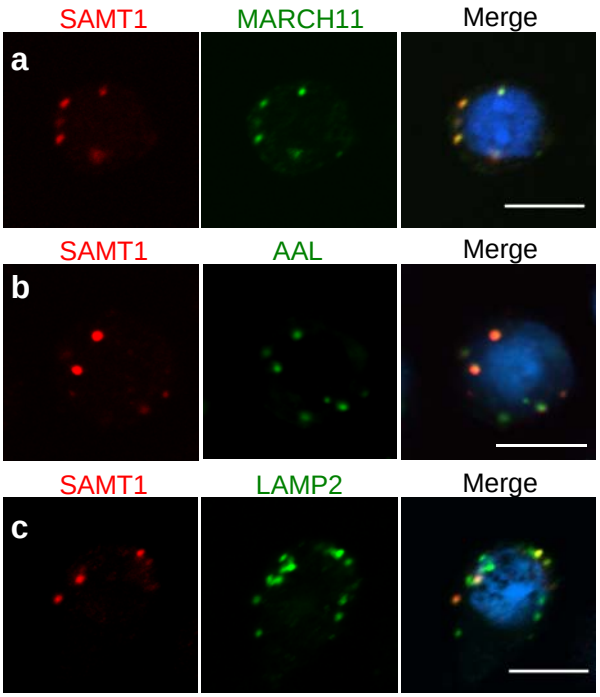

Fig. 6

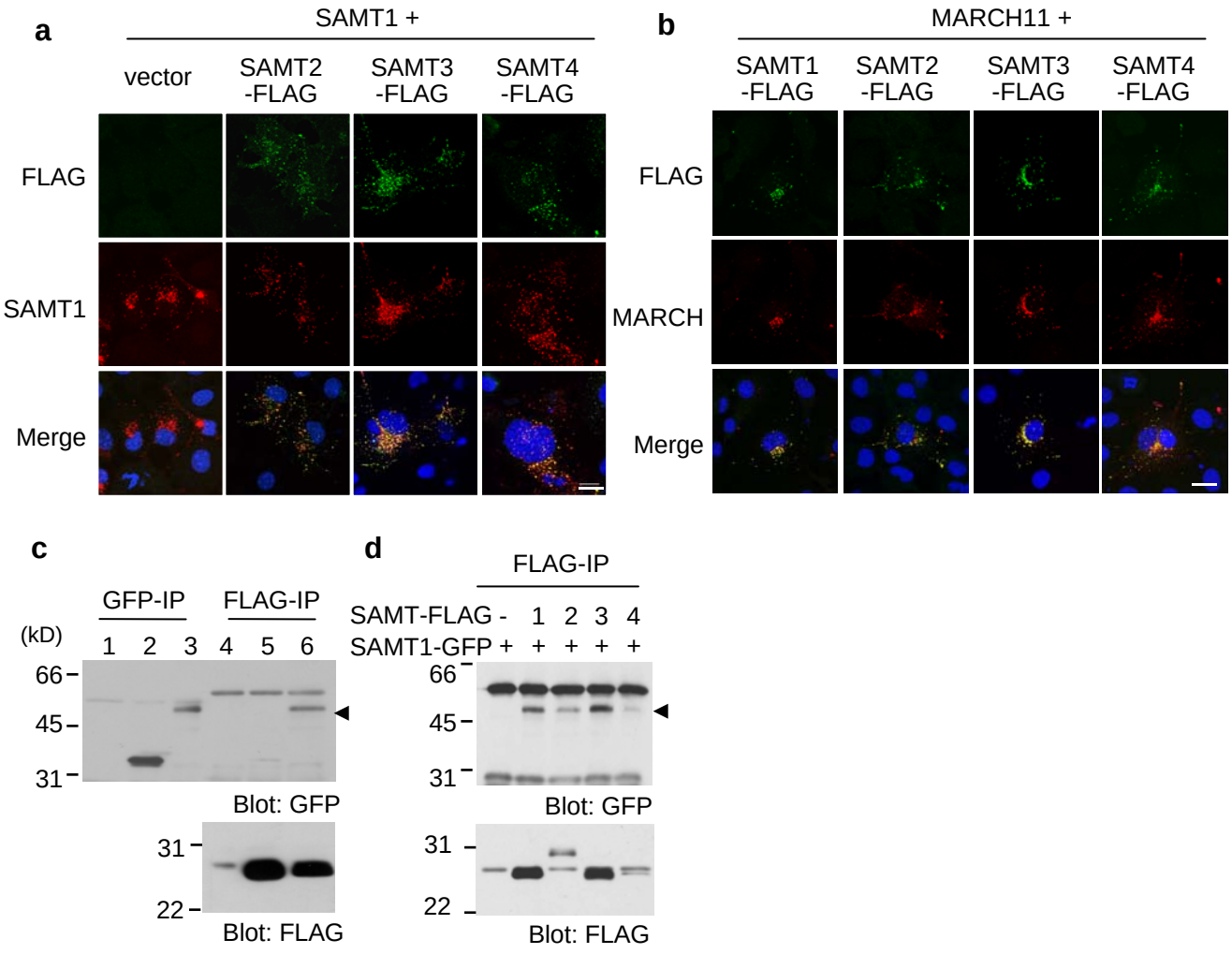
a
SAMT1 +
vector
SAMT2 -FLAG
SAMT3 -FLAG
SAMT4 -FLAG
FLAG
SAMT1
Merge
b
MARCH11 +
SAMT1 -FLAG
SAMT2 -FLAG
SAMT3 -FLAG
SAMT4 -FLAG
FLAG
MARCH
Merge
c
GFP-IP
FLAG-IP
(kD)
1 2 3 4 5 6
66
45
31
Blot: GFP
31
22
Blot: FLAG
d
FLAG-IP
SAMT-FLAG - 1 2 3 4
SAMT1-GFP + + + + +
66
45
31
Blot: GFP
31
22
Blot: FLAG

Fig. 7

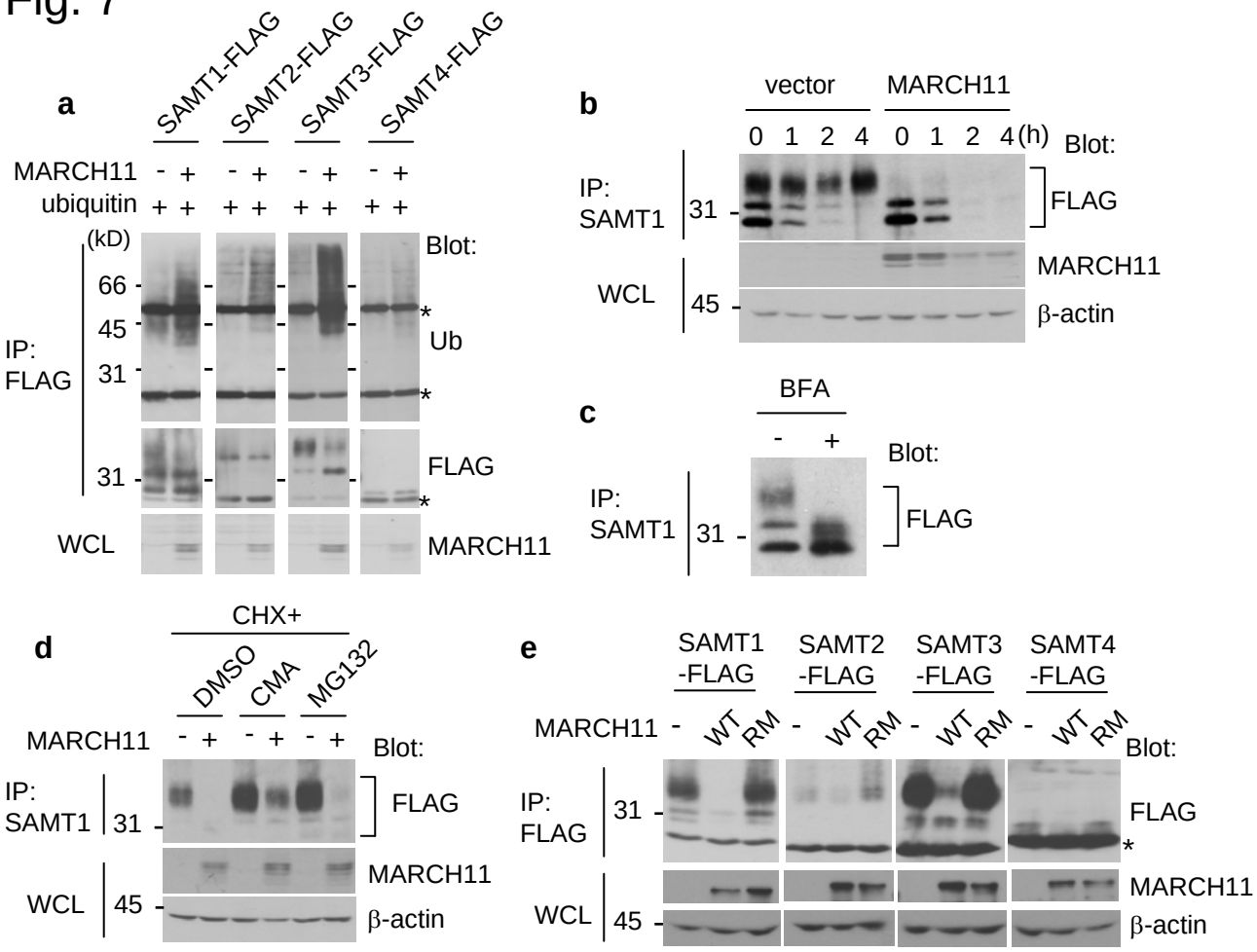
a
SAMT1-FLAG
SAMT2-FLAG
SAMT3-FLAG
SAMT4-FLAG
MARCH11 - + - + - + - +
ubiquitin + + + + + + + +
(kD)
66
45
31
IP: FLAG
Blot:
Ub
FLAG
WCL
MARCH11
b
vector
MARCH11
0 1 2 4 0 1 2 4 (h)
Blot:
IP: SAMT1
31
FLAG
MARCH11
WCL
45
β-actin
c
BFA
- +
Blot:
IP: SAMT1
31
FLAG
d
CHX+
DMSO
CMA
MG132
MARCH11 - + - + - +
Blot:
IP: SAMT1
31
FLAG
MARCH11
WCL
45
β-actin
e
SAMT1 -FLAG
SAMT2 -FLAG
SAMT3 -FLAG
SAMT4 -FLAG
MARCH11 - WT RM - WT RM - WT RM - WT RM
Blot:
IP: FLAG
31
FLAG
MARCH11
WCL
45
β-actin

Fig. 8

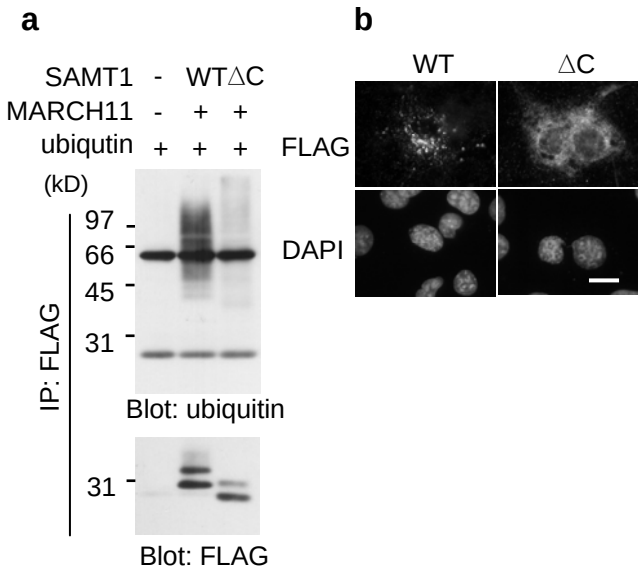
a
SAMT1 - WTΔC
MARCH11 - + +
ubiqutin + + +
(kD)
97
66
45
31
IP: FLAG
Blot: ubiquitin
31
Blot: FLAG
b
WT
ΔC
FLAG
DAPI

loading control. **c** 293 cells expressing SAMT1-FLAG were treated with or without 5 μg/ml brefeldin A (BFA) for 6 h and SAMT1 expression was monitored as in b. **d** SAMT1-FLAG was expressed in 293F cells with or without MARCH11, and the cells were treated with cycloheximide (CHX) combined with solvent (DMSO), 50 nM concanamycin A (CMA), or 20 μM MG132 for 4 h. The expression of SAMT1 and MARCH11 was monitored as in b. **e** SAMT1–SAMT4 were expressed in 293F cells with wild-type (WT) or RING-finger mutant (RM) of MARCH11. After 4 h of treatment with cycloheximide, cell lysates were collected, and the expression of SAMT1–SAMT4 and MARCH11 was monitored similarly

Fig. 8 Effect of deletion of the C-terminal region of SAMT1 on its ubiquitination and intracellular localization

a FLAG-tagged wild-type (WT) and a C-terminal deletion mutant (ΔC) of SAMT1 were introduced into 293F cells, and ubiquitination levels were analyzed by immunoprecipitation and western blotting. **b** FLAG-tagged wild-type (WT) and a C-terminal deletion mutant (ΔC) of SAMT1 were introduced into COS7 cells, and their intracellular localization was analyzed with immunofluorescence staining using anti-FLAG antibody (top panel). Nuclei were visualized with DAPI (bottom panel). Bar, 10 μm